

## **Supplemental materials**

Combating carbapenem-resistant *Acinetobacter baumannii* by an optimized imipenem plus tobramycin dosage regimen – prospective validation *via* hollow fiber infection and mathematical modeling, by Landersdorfer CB *et al.*

## **Materials and methods**

### ***Bacterial isolate and susceptibility testing***

The clinical CRAB isolate (FADDI-AB034; MIC<sub>Imipenem</sub>: 32 mg/liter and MIC<sub>Tobramycin</sub>: 2 mg/liter) was obtained from the collection at Monash University. All *in vitro* studies used cation-adjusted Mueller Hinton Broth (CAMHB; BBL™, BD, Sparks, MD). Drug-containing agar plates were freshly prepared on the same day by adding imipenem or tobramycin to cation-adjusted Mueller Hinton agar (CAMHA; BD, Sparks, MD, USA). Preparation of antibiotic stock solutions, viable counting, and MIC testing were performed as described previously (1) following CLSI guidelines (2). We used EUCAST breakpoints (3).

### ***Dynamic hollow fiber in vitro infection model***

A HFIM, as previously described (4, 5), was used to simulate the time-course of antibiotic concentrations as expected in patients for the proposed dosage regimen. In brief, cellulosic cartridges (model: C3008, Batch No. B720170715b; FiberCell Systems Inc., Frederick, MD, USA) were used and the HFIM system was maintained at 36 °C in a humidified incubator. The target inoculum was  $10^{7.2}$  CFU/mL. We targeted an inoculum of  $\sim 10^7$  CFU/mL as has been previously used in HFIM studies (6, 7), to mirror bacterial densities in severe infections in patients (8, 9). The viable count samples were collected at 0, 1.5, 4, 8, 23, 25.5, 28, 47, 52, 71, 95, 119, 143 and 166h. All bacterial samples were washed twice to prevent antibiotic carryover *via* centrifugation (5 min at 4000 × g) and resuspension in sterile saline. Viable counts for the total population were determined by

manual plating of 100  $\mu\text{L}$  of an undiluted or appropriately diluted suspension in saline onto CAMHA plates (4, 10, 11). For samples with low viable counts, 200  $\mu\text{L}$  were plated. This technique yields a limit of counting (equivalent to 1 colony per plate) of 1.0 or 0.7  $\log_{10}$  (CFU/mL). Pharmacokinetic samples were collected at various time points over multiple days and stored at  $-80^{\circ}\text{C}$  prior to LC-MS/MS analysis of drug concentrations.

### ***Mutant frequencies and emergence of resistance***

To characterize the emergence of resistance, mutant frequencies were determined at pre-dose (*i.e.* 0h) and at 4, 23, 47, 71, 95, and 143h. Resistant bacteria were quantified by plating 200  $\mu\text{L}$  of washed bacterial samples on agar plates supplemented with imipenem at 1.75 $\times$  and 3 $\times$  MIC (*i.e.* 56 and 96 mg/liter imipenem), or tobramycin at 3 $\times$  and 5 $\times$  MIC (*i.e.* 6 and 10 mg/liter tobramycin). Agar plates were incubated for 2 days and mutant frequencies calculated as the difference between the  $\log_{10}$  CFU/mL on antibiotic-containing agar plates and the  $\log_{10}$  CFU/mL on drug-free plates at the same time.

### ***Experimental design and simulated imipenem and tobramycin dosage regimens***

We simulated in the HFIM a continuous infusion of imipenem 4 g/day with 1 g loading dose at 0h to rapidly achieve steady state. For tobramycin the dosage regimen was 7 mg/kg as 0.5h infusion every 24h; tobramycin was dosed with a high-precision New Era syringe pump. All simulated antibiotic concentration-time profiles in the HFIM were predicted *via* Monte Carlo simulations based on published population pharmacokinetic models in critically-ill patients (1, 12, 13). For imipenem the total body clearance was 11.1 L/h, volume of distribution 12.2 L, half-life 0.8 h, and unbound fraction in plasma 0.91 (13). For tobramycin, total body clearance was 3.83 L/h, volume of distribution of the central compartment 25.5 L, volume of distribution of the peripheral compartment 30.6 L,

inter-compartmental distribution clearance 4.74 L/h, and unbound fraction in plasma 1.0 (12). The experimental design consisted of one growth control, one tobramycin monotherapy, three treatment arms reflecting imipenem monotherapy, and all three combinations of imipenem plus tobramycin. While HFIM studies were run as a single replicate, we assessed a range of imipenem concentrations. The three imipenem concentration-time profiles represent the median, the 5<sup>th</sup> and the 95<sup>th</sup> percentile of the expected unbound plasma concentrations arising from a 4 g/day continuous infusion with 1 g loading dose. The loading dose was given as a bolus into the central reservoir of the HFIM. To achieve the targeted constant imipenem concentrations following a continuous infusion, imipenem was directly added to the inflowing reservoirs of the HFIM; the latter were kept at 4°C during the experiment and changed every 24h.

### ***Bioanalysis***

Antibiotic concentrations in CAMHB were determined by a liquid chromatography tandem mass spectrometry (LC-MS/MS) assay. An Agilent 1200 HPLC coupled with an Agilent 6430 triple-quadrupole mass spectrometer equipped with a turbo ion electrospray ionization (ESI) source (Agilent Technologies, Santa Clara, CA) was used for analysis.

To determine tobramycin, a portion (50 µL) of the internal standard (IS) solution (10 µg/mL of metformin in acetonitrile) was spiked to 50 µL of samples and vortex-mixed for 30 sec. Then, 50 µL of acetonitrile and 100 µL of 0.05% trichloroacetic acid were added and the tube contents vortex-mixed for 1 min. After centrifugation of the mixture for 10 min at 15,000 × g, 100 µL of the supernatant was transferred to a polypropylene HPLC vial and mixed with 100 µL of distilled water. The mixture was vortex-mixed for 30 sec and a portion (5 µL) was injected into the LC-MS/MS. Tobramycin, imipenem and the

IS were separated on a Synergi Polar-RP column (150 × 2.0 mm, 4.0 μm) (Phenomenex, Torrance, CA, USA) using a binary gradient mobile phase composed of 0.25% formic acid (A) and acetonitrile (B) programmed as A:B = 80:20 (0-1 and 3.6-10 min) and A:B = 10:90 (1.1-3.5 min). The flow rate of the mobile phase was 0.2 mL/min (0-2.5 and 4.9-10.0 min) and 0.5 mL/min (2.6-4.8 min). The column oven temperature was 30°C and the total run time 10 min.

The ESI source was operated in a positive mode and the ionization gas temperature was set at 350°C. The mass transitions of the precursor → product ion pairs were monitored at m/z of 468.3→163.1 for tobramycin and 130.1→71.0 for metformin. The mass spectrometric data were processed by the MassHunter Quantitative Analysis software (Agilent Technologies, Santa Clara, CA, USA). The lower limit of quantification (LLOQ) was 0.050 mg/liter and the correlation coefficient was greater than 0.99. The precision was within 11.6% and accuracy within 4% at 0.150, 2.00 and 20.0 mg/liter.

### ***Mechanism-based population PK/PD modeling***

Mechanism-based PK/PD modeling (MBM) was performed to characterize the time-course of bacterial killing and regrowth. All unbound drug concentrations and viable counts were fitted simultaneously utilizing the S-ADAPT software (version 1.57) with the importance sampling algorithm (pmethod=4) (14, 15). SADAPT-TRAN was used for pre- and post-processing (16). Competing models were evaluated as described previously (17, 18).

***Life-cycle growth model:*** A life-cycle growth model was utilized to describe bacterial replication (19, 20) (**Fig. S3**). The first-order growth rate constant ( $k_{12}$ ) determines the mean generation time (MGT) and reflects the transition from the

vegetative state (*i.e.* state 1) to the replicating state (*i.e.* state 2). The  $k_{21}$  was set to  $50 \text{ h}^{-1}$ , since replication was assumed to be fast (20). Informed by our previously developed MBM (1), the final model included three pre-existing bacterial subpopulations of different susceptibility to imipenem and tobramycin (**Fig. S4**). Each subpopulation was described by the two states (*i.e.* compartments). The total concentration of viable bacteria ( $\text{CFU}_{\text{All}}$ ) was:

$$\text{CFU}_{\text{All}} = \text{CFU}_{\text{SS1}} + \text{CFU}_{\text{SS2}} + \text{CFU}_{\text{RI1}} + \text{CFU}_{\text{RI2}} + \text{CFU}_{\text{IR1}} + \text{CFU}_{\text{IR2}} \quad (1)$$

The  $\text{CFU}_{\text{NN},\#}$  described the concentration of viable bacteria for population NN in state 1 or 2.

**Bacterial killing:** The rates of bacterial killing by imipenem and tobramycin monotherapy were faster than the rate of growth. Therefore, we specified killing *via* one direct killing process each for imipenem and tobramycin. The differential equation for the double susceptible population in state 1 ( $\text{CFU}_{\text{SS1}}$ ) comprised killing by imipenem (concentration:  $C_{\text{IPM}}$ ) and tobramycin ( $C_{\text{TOB}}$ ; initial conditions, model parameters and variables are described below and in Table 2):

$$\frac{d(\text{CFU}_{\text{SS1}})}{dt} = 2 \cdot \text{PLAT} \cdot k_{21} \cdot \text{CFU}_{\text{SS2}} - k_{12\text{SS}} \cdot \text{CFU}_{\text{SS1}} - \left( \frac{K_{\text{max,IPM}} \cdot C_{\text{IPM}}^{\text{Hill}_{\text{IPM}}}}{C_{\text{IPM}}^{\text{Hill}_{\text{IPM}}} + \text{KC}_{50,\text{SS,IPM}}^{\text{Hill}_{\text{IPM}}}} + \frac{K_{\text{max,SS,TOB}} \cdot C_{\text{TOB}}}{C_{\text{TOB}} + \text{KC}_{50,\text{SS,TOB}}} \right) \cdot \text{CFU}_{\text{SS1}} \quad (2)$$

The  $\text{CFU}_{\text{SS2}}$  is the bacterial concentration of the double susceptible population in state 2. The plateau factor (PLAT) represents the probability of successful replication and is defined as described previously (1, 11, 21). The  $K_{\text{max}}$  is the maximum killing rate constant,  $\text{KC}_{50}$  is the associated antibiotic concentration causing 50% of  $K_{\text{max}}$  and  $\text{Hill}_{\text{IPM}}$  is the Hill coefficient for imipenem (**Fig. S4**). Imipenem and tobramycin were assumed to

kill the bacteria in both states, thus the same killing functions were used for states 1 and 2. The differential equation of the double susceptible population in state 2 (CFU<sub>SS2</sub>) was:

$$\frac{d(\text{CFU}_{\text{SS2}})}{dt} = -k_{21} \cdot \text{CFU}_{\text{SS2}} + k_{12\text{ss}} \cdot \text{CFU}_{\text{SS1}} - \left( \frac{K_{\text{max,IPM}} \cdot C_{\text{IPM}}^{\text{Hill}_{\text{IPM}}}}{C_{\text{IPM}}^{\text{Hill}_{\text{IPM}}} + \text{KC}_{50,\text{SS,IPM}}^{\text{Hill}_{\text{IPM}}}} + \frac{K_{\text{max,SS,TOB}} \cdot C_{\text{TOB}}}{C_{\text{TOB}} + \text{KC}_{50,\text{SS,TOB}}} \right) \cdot \text{CFU}_{\text{SS2}} \quad (3)$$

The differential equations for the other two populations (RI and IR) had the same structure as the equations for the double susceptible population, but included different estimates for  $K_{\text{max,TOB}}$ ,  $\text{KC}_{50}$  and  $k_{12}$  compared to the double susceptible population.

**Synergy modeling:** The MBM utilized a life-cycle growth model to describe the underlying biology of bacterial replication (19, 20). Informed by our previously developed MBM (1), the final model included three pre-existing bacterial subpopulations; a double-susceptible (IPM<sup>S</sup>/TOB<sup>S</sup>), an imipenem-resistant tobramycin-intermediate (IPM<sup>R</sup>/TOB<sup>I</sup>), and an imipenem-intermediate tobramycin-resistant (IPM<sup>I</sup>/TOB<sup>R</sup>) bacterial population (**Fig. S3 and Fig. S4**). We evaluated two potential types of synergy: 1) ‘subpopulation synergy’, where imipenem kills the tobramycin-resistant subpopulation and *vice versa*, and 2) mechanistic synergy, which occurs with tobramycin enhancing the killing by imipenem. Mechanistic synergy was incorporated in the model by assuming an increase in the target site penetration of imipenem due to disruption of the outer membrane by tobramycin (22, 23). This was implemented by estimating (*via* an IF-condition statement) a lower  $\text{KC}_{50,\text{IPM}}$  (*i.e.* imipenem concentration required to yield half-maximal killing) in the presence of an estimated threshold tobramycin concentration.

**Parameter variability and residual error model**

The between curve variability of the model parameters was assumed to be log-normally distributed, except for parameters constrained between 0 and 1 that were logistically transformed, as described previously (1). The residual error model was the same as we described previously (1, 10, 19, 21, 24).

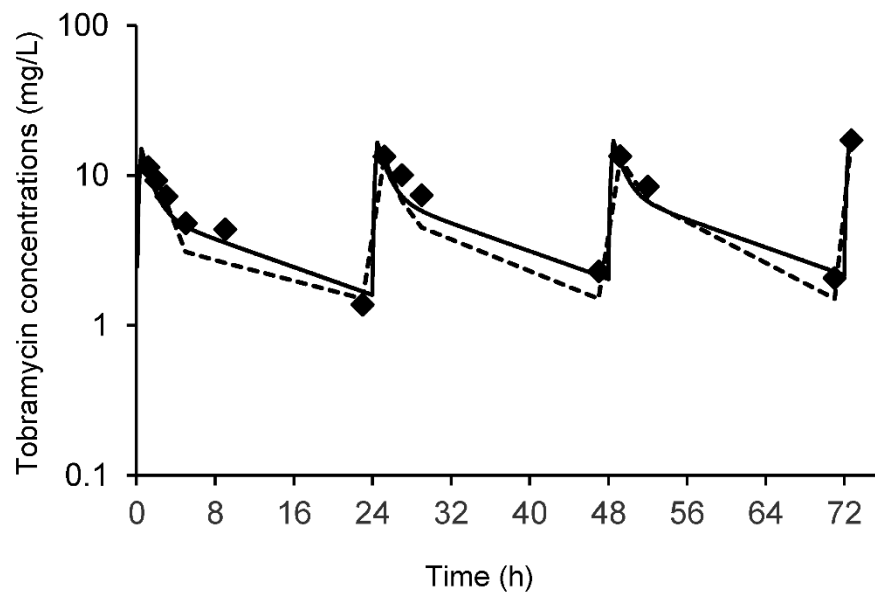


**Figure S1:** Comparison of targeted (broken lines), observed (markers), and population model fitted (continuous lines) tobramycin concentrations in the dynamic *in vitro* hollow fiber infection model.

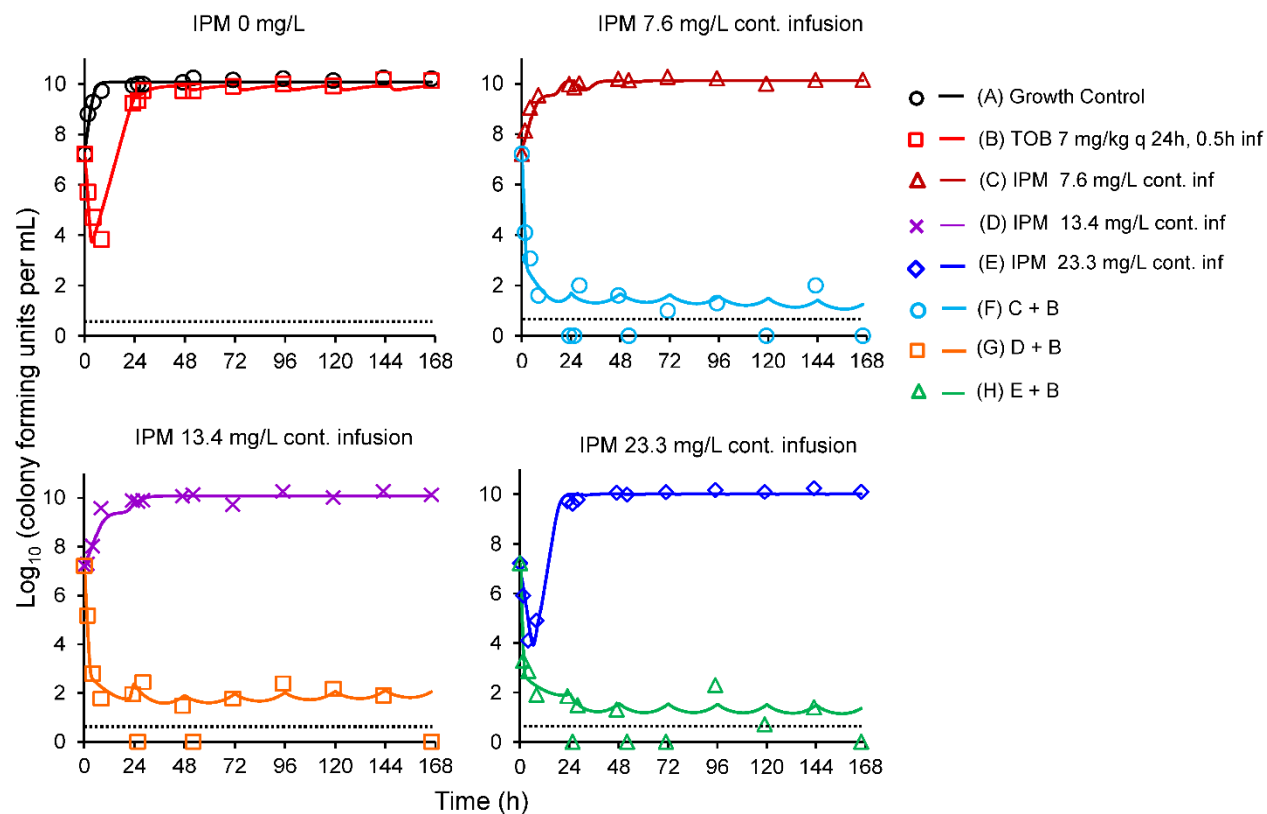


**Figure S2:** Observed (markers) and individual MBM-fitted (lines) viable count profiles for imipenem, tobramycin and their combination against CRAB isolate FADDI-AB034. Imipenem 7.6 mg/liter (low; 5<sup>th</sup> percentile), 13.4 mg/liter (intermediate; median) and 23.3 mg/liter (high; 95<sup>th</sup> percentile) are three clinically relevant imipenem concentrations arising from 4 g/day continuous infusion with a 1 g loading dose. These concentration profiles were simulated in the dynamic *in vitro* HFIM. Observed viable counts below the limit of counting (*i.e.* below 0.7  $\text{log}_{10}$  CFU/mL; dashed horizontal line) were plotted as zero.



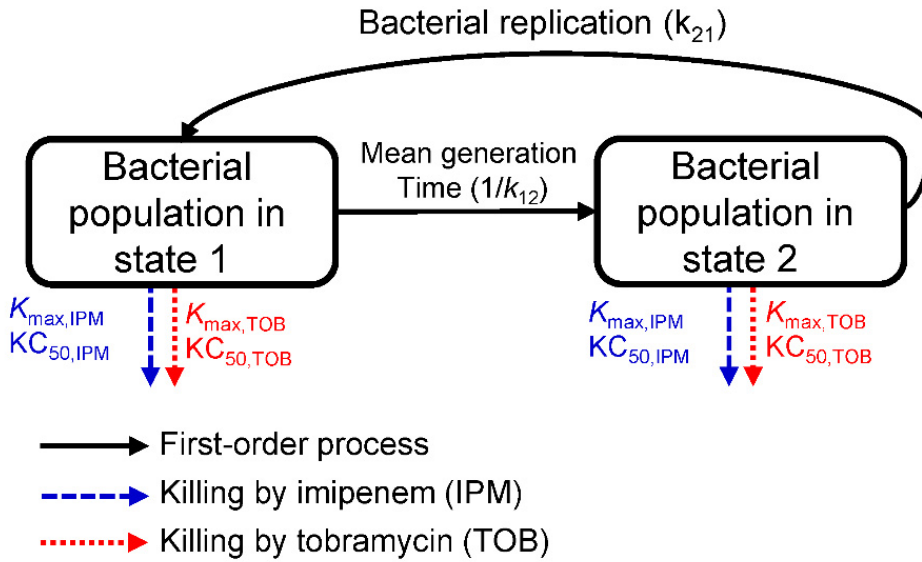


**Figure S3:** Life cycle growth model utilized for each of the three populations to describe bacterial replication.

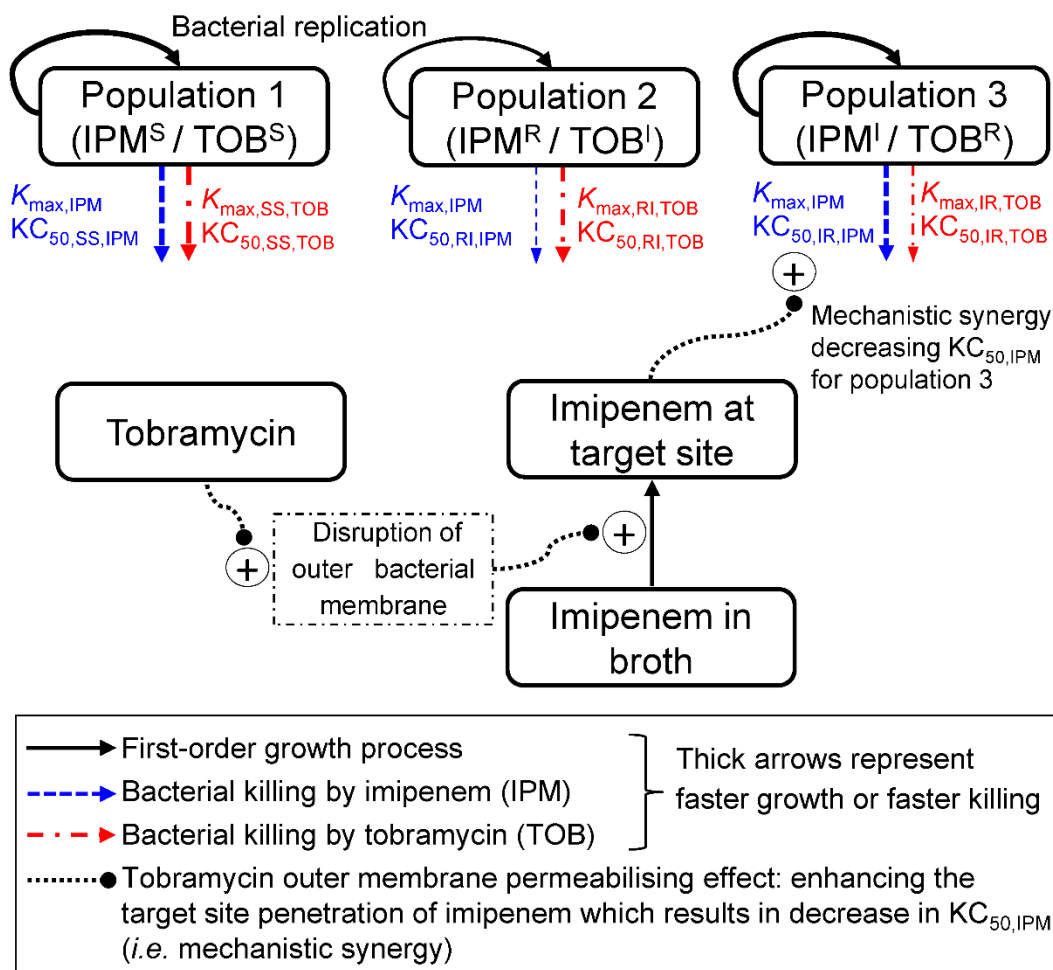


**Figure S4:** The structure of the mechanism-based model for bacterial growth and killing by imipenem and tobramycin in monotherapies and combination. The IPM<sup>S</sup>/TOB<sup>S</sup> population is susceptible to both imipenem and tobramycin, the IPM<sup>R</sup>/TOB<sup>I</sup> population is imipenem resistant and has intermediate susceptibility to tobramycin, and the IPM<sup>I</sup>/TOB<sup>R</sup> population is tobramycin resistant and has intermediate susceptibility to imipenem. The maximum killing rate constants ( $K_{max}$ ) and the associated antibiotic concentrations ( $KC_{50}$ ) causing 50% of  $K_{max}$  are explained in Table 1. Mechanistic synergy (*i.e.* tobramycin enhancing the target site penetration of imipenem) was identified and included for population 3.

**Table S1.** Log<sub>10</sub> mutant frequencies at 56 and 96 mg/liter imipenem (1.75× and 3× the baseline MIC) and at 6 and 10 mg/liter tobramycin (3× and 5× the baseline MIC) at various time points for each treatment arm simulated in the HFIM. <sup>a</sup>

Antibiotic containing agar plates	Time (h)	Control	TOB 7 mg/kg q24h	IPM 7.6 mg/liter cont. inf	IPM 13.4 mg/liter cont. inf	IPM 23.3 mg/liter cont. inf	IPM 7.6 mg/liter cont. inf + TOB 7 mg/kg	IPM 13.4 mg/liter cont. inf + TOB 7 mg/kg	IPM 23.3 mg/liter cont. inf + TOB 7 mg/kg
56 mg/L IPM (1.75× MIC)	0	-6.51	-	-6.51	-6.51	-6.51	-6.51	-6.51	-6.51
	4	-5.76	-	-5.74	-5.07	< -4.09	< -3.08	< -2.79	< -2.86
	23	-6.16	-	-5.73	-6.10	-1.83	< 0	< -1.95	< -1.85
	47	-6.28	-	-5.84	-5.62	-2.55	< -1.60	< -1.48	< -1.30
	71	-5.68	-	-5.79	-4.99	-2.87	< -1	< -1.78	< 0
	95	-6.91	-	-5.60	-5.40	-2.60	< -1.30	< -2.39	< -2.29
	143	-5.90	-	-5.74	-5.71	-3.67	< -2	< -1.90	< -1.40
96 mg/L IPM (3× MIC)	0	-7.21	-	-7.21	-7.21	-7.21	-7.21	-7.21	-7.21
	4	< -9.28	-	-6.74	-4.65	< -4.09	< -3.08	< -2.79	< -2.86
	23	-5.37	-	-5.52	-6.08	-3.87	< 0	< -1.95	< -1.85
	47	-5.96	-	-6.34	-7.05	-4.97	< -1.60	< -1.48	< -1.30
	71	-6.84	-	-6.67	-5.86	-4.88	< -1	< -1.78	< 0
	95	-6.74	-	-6.60	-6.13	-4.26	< -1.30	< -2.39	< -2.29
	143	-6.17	-	-6.24	-6.22	-5.43	< -2	< -1.90	< -1.40
6 mg/L TOB (3× MIC)	0	< -7.21	< -7.21	-	-	-	< -7.21	< -7.21	< -7.21
	4	-7.58	< -4.70	-	-	-	< -3.08	< -2.79	< -2.86
	23	-7.35	-1.94	-	-	-	< 0	< -1.95	< -1.85
	47	-7.60	-2.25	-	-	-	< -1.60	< -1.48	< -1.30
	71	-7.09	-1.39	-	-	-	< -1	< -1.78	< 0
	95	-7.27	-0.36	-	-	-	< -1.30	< -2.39	< -2.29
	143	-7.79	-0.93	-	-	-	-0.22	-0.12	0.08
10 mg/L TOB (5× MIC)	0	< -7.21	< -7.21	-7.21	-7.21	-7.21	< -7.21	< -7.21	< -7.21
	4	< -9.28	< -4.70	-6.74	-4.65	< -4.09	< -3.08	< -2.79	< -2.86
	23	-8.16	-5.34	-5.52	-6.08	-3.87	< 0	< -1.95	< -1.85
	47	-8.06	-1.65	-6.34	-7.05	-4.97	< -1.60	< -1.48	< -1.30
	71	-8.46	-1.53	-6.67	-5.86	-4.88	< -1	< -1.78	< 0
	95	-8.91	-0.89	-6.60	-6.13	-4.26	< -1.30	< -2.39	-1.29
	143	-8.94	-1.31	-6.24	-6.22	-5.43	-1.00	< -1.90	< -1.40

<sup>a</sup> Imipenem 7.6 mg/liter (low; 5<sup>th</sup> percentile), 13.4 mg/liter (intermediate; median) and 23.3 mg/liter (high; 95<sup>th</sup> percentile) are 3 clinically relevant imipenem profiles arising from 4g/day continuous infusion with 1g loading dose.  
 -: Viable counts on drug plate for this antibiotic not assessed for the respective regimen.

## References

1. Yadav R, Landersdorfer CB, Nation RL, Boyce JD, Bulitta JB. 2015. Novel approach to optimize synergistic carbapenem-aminoglycoside combinations against carbapenem-resistant *Acinetobacter baumannii*. *Antimicrob Agents Chemother* 59:2286-2298. <https://doi.org/10.1128/aac.04379-14>.
2. Anonymous. 2015. Clinical and Laboratory Standards Institute. Performance Standards for Antimicrobial Susceptibility Testing: 25th Informational Supplement. M100-S125. Wayne, PA, USA: CLSI.
3. Anonymous. 2015. European Committee on Antimicrobial Susceptibility Testing. Breakpoint Tables for Interpretation of MICs and Zone Diameters, Version 5.0; <http://www.eucast.org>.
4. Nicasio AM, Bulitta JB, Lodise TP, D'Hondt RE, Kulawy R, Louie A, Drusano GL. 2012. Evaluation of once-daily vancomycin against methicillin-resistant *Staphylococcus aureus* in a hollow-fiber infection model. *Antimicrob Agents Chemother* 56:682-686. <https://doi.org/10.1128/AAC.05664-11>.
5. Tsuji BT, Bulitta JB, Brown T, Forrest A, Kelchlin PA, Holden PN, Peloquin CA, Skerlos L, Hanna D. 2012. Pharmacodynamics of early, high-dose linezolid against vancomycin-resistant enterococci with elevated MICs and pre-existing genetic mutations. *J Antimicrob Chemother* 67:2182-2190. <https://doi.org/10.1093/jac/dks201>.
6. Li X, Wang L, Zhang XJ, Yang Y, Gong WT, Xu B, Zhu YQ, Liu W. 2014. Evaluation of meropenem regimens suppressing emergence of resistance in *Acinetobacter baumannii* with human simulated exposure in an in vitro intravenous-infusion hollow-fiber infection model. *Antimicrob Agents Chemother* 58:6773-6781. <https://doi.org/10.1128/aac.03505-14>.
7. Tam VH, Schilling AN, Neshat S, Poole K, Melnick DA, Coyle EA. 2005. Optimization of meropenem minimum concentration/MIC ratio to suppress in vitro resistance of *Pseudomonas aeruginosa*. *Antimicrob Agents Chemother* 49:4920-4927. <https://doi.org/10.1128/aac.49.12.4920-4927.2005>.
8. Konig C, Simmen HP, Blaser J. 1998. Bacterial concentrations in pus and infected peritoneal fluid--implications for bactericidal activity of antibiotics. *J Antimicrob Chemother* 42:227-232.
9. Lee S, Kwon KT, Kim HI, Chang HH, Lee JM, Choe PG, Park WB, Kim NJ, Oh MD, Song DY, Kim SW. 2014. Clinical Implications of Cefazolin Inoculum Effect and  $\beta$ -Lactamase Type on Methicillin-Susceptible *Staphylococcus aureus* Bacteremia. *Microb Drug Resist* 20:568-574.
10. Bulitta JB, Yang JC, Yohann L, Ly NS, Brown SV, D'Hondt RE, Jusko WJ, Forrest A, Tsuji BT. 2010. Attenuation of colistin bactericidal activity by high inoculum of *Pseudomonas aeruginosa* characterized by a new mechanism-based population pharmacodynamic model. *Antimicrob Agents Chemother* 54:2051-2062. <https://doi.org/10.1128/AAC.00881-09>.
11. Landersdorfer CB, Ly NS, Xu H, Tsuji BT, Bulitta JB. 2013. Quantifying subpopulation synergy for antibiotic combinations via mechanism-based modeling and a sequential dosing design. *Antimicrob Agents Chemother* 57:2343-2351. <https://doi.org/10.1128/AAC.00092-13>.

12. Conil JM, Georges B, Ruiz S, Rival T, Seguin T, Cougot P, Fourcade O, Pharmd GH, Saivin S. 2011. Tobramycin disposition in ICU patients receiving a once daily regimen: population approach and dosage simulations. *Br J Clin Pharmacol* 71:61-71. <https://doi.org/10.1111/j.1365-2125.2010.03793.x>.
13. Sakka SG, Glauner AK, Bulitta JB, Kinzig-Schippers M, Pfister W, Drusano GL, Sorgel F. 2007. Population Pharmacokinetics and Pharmacodynamics of Continuous versus Short-Term Infusion of Imipenem-Cilastatin in Critically Ill Patients in a Randomized, Controlled Trial. *Antimicrob Agents Chemother* 51:3304-3310.
14. Bauer RJ, Guzy S, Ng C. 2007. A survey of population analysis methods and software for complex pharmacokinetic and pharmacodynamic models with examples. *AAPS J* 9:E60-83.
15. Bulitta JB, Landersdorfer CB. 2011. Performance and robustness of the Monte Carlo importance sampling algorithm using parallelized S-ADAPT for basic and complex mechanistic models. *AAPS J* 13:212-226. <https://doi.org/10.1208/s12248-011-9258-9>.
16. Bulitta JB, Bingolbali A, Shin BS, Landersdorfer CB. 2011. Development of a new pre- and post-processing tool (SADAPT-TRAN) for nonlinear mixed-effects modeling in S-ADAPT. *AAPS J* 13:201-211. <https://doi.org/10.1208/s12248-011-9257-x>.
17. Bulitta JB, Duffull SB, Kinzig-Schippers M, Holzgrabe U, Stephan U, Drusano GL, Sorgel F. 2007. Systematic comparison of the population pharmacokinetics and pharmacodynamics of piperacillin in cystic fibrosis patients and healthy volunteers. *Antimicrob Agents Chemother* 51:2497-2507.
18. Tsuji BT, Okusanya OO, Bulitta JB, Forrest A, Bhavnani SM, Fernandez PB, Ambrose PG. 2011. Application of pharmacokinetic-pharmacodynamic modeling and the justification of a novel fusidic acid dosing regimen: raising Lazarus from the dead. *Clin Infect Dis* 52 Suppl 7:S513-519. <https://doi.org/10.1093/cid/cir166>.
19. Bulitta JB, Ly NS, Yang JC, Forrest A, Jusko WJ, Tsuji BT. 2009. Development and qualification of a pharmacodynamic model for the pronounced inoculum effect of ceftazidime against *Pseudomonas aeruginosa*. *Antimicrob Agents Chemother* 53:46-56. <https://doi.org/10.1128/AAC.00489-08>.
20. Maidhof H, Johannsen L, Labischinski H, Giesbrecht P. 1989. Onset of penicillin-induced bacteriolysis in staphylococci is cell cycle dependent. *J Bacteriol* 171:2252-2257.
21. Yadav R, Bulitta JB, Nation RL, Landersdorfer CB. 2017. Optimization of Synergistic Combination Regimens against Carbapenem- and Aminoglycoside-Resistant Clinical *Pseudomonas aeruginosa* Isolates via Mechanism-Based Pharmacokinetic/Pharmacodynamic Modeling. *Antimicrob Agents Chemother* 61. <https://doi.org/10.1128/aac.01011-16>.
22. Kadurugamuwa JL, Clarke AJ, Beveridge TJ. 1993. Surface action of gentamicin on *Pseudomonas aeruginosa*. *J Bacteriol* 175:5798-5805.
23. Kadurugamuwa JL, Lam JS, Beveridge TJ. 1993. Interaction of gentamicin with the A band and B band lipopolysaccharides of *Pseudomonas aeruginosa* and its possible lethal effect. *Antimicrob Agents Chemother* 37:715-721.
24. Bulitta JB, Ly NS, Landersdorfer CB, Wanigaratne NA, Velkov T, Yadav R, Oliver A, Martin L, Shin BS, Forrest A, Tsuji BT. 2015. Two mechanisms of killing of *Pseudomonas aeruginosa* by tobramycin assessed at multiple inocula via mechanism-based modeling. *Antimicrob Agents Chemother* 59:2315-2327. <https://doi.org/10.1128/aac.04099-14>.